

Supporting Information

Highly efficient TADF OLEDs with low efficiency roll-off based on novel acridine–carbazole hybrid donor-substituted pyrimidine derivatives

Qing Zhang^a, Shuaiqiang Sun^a, Won Jae Chung^b Sung Joon Yoon^b, Yaxiong Wang^a, Runda Guo^a, Shaofeng Ye^a, Jun Yeob Lee^{*b}, Lei Wang^{*a}

^a Wuhan National Laboratory for Optoelectronics, Huazhong University of Science and Technology, Wuhan, 430074, P. R. China
E-mail: wanglei@mail.hust.edu.cn

^b School of Chemical Engineering, Sungkyunkwan University, Suwon, Gyeonggi, 440-746, Republic of Korea. E-mail: leej17@skku.edu;

Transient PL characteristics, fabrication and performance measurement for DPEPO-hosted devices were the same as the reports.¹⁻³ Apart from the above experiment, the computational details and measurement instruments were cited by our previous work.⁴⁻⁶

The evaluation of exciton dynamic rate constants was calculated by equation S1-S7:

$$k_{PF} = \frac{\phi_{PF}}{\tau_P} \quad \text{Equation S1}$$

$$k_{DF} = \frac{\phi_{DF}}{\tau_D} \quad \text{Equation S2}$$

$$k_{ISC} = \frac{\phi_{DF}}{\phi_{PF} + \phi_{DF}} k_{PF} \quad \text{Equation S3}$$

$$k_{RISC} = \frac{k_{DF} k_{PF} \phi_{DF}}{k_{ISC} \phi_{PF}} \quad \text{Equation S4}$$

$$k_{PF} = k_r^S + k_{nr}^S + k_{ISC} \quad \text{Equation S5}$$

$$\phi_{PF} = \frac{k_r^S}{k_r^S + k_{nr}^S + k_{ISC}} = \frac{k_r^S}{k_{PF}} \quad \text{Equation S6}$$

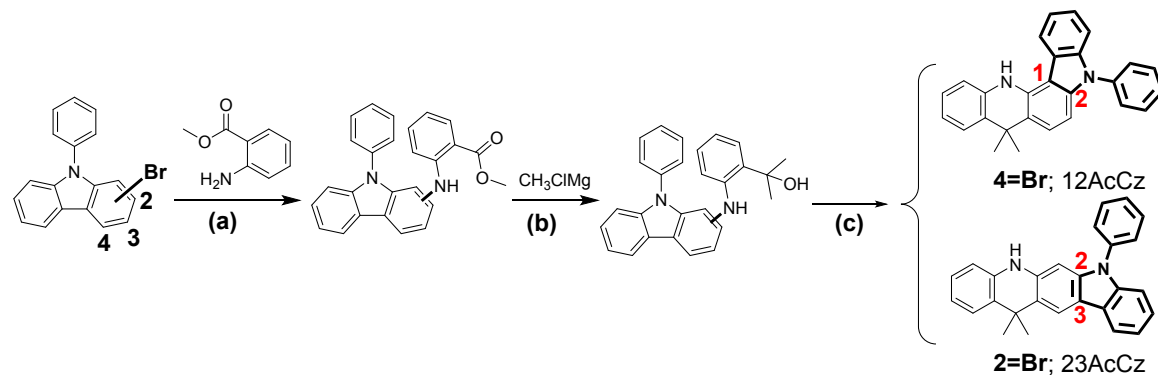
$$\phi_{ISC} = \frac{k_{ISC}}{k_r^S + k_{nr}^S + k_{ISC}} = \frac{k_{ISC}}{k_{PF}} \quad \text{Equation S7}$$

Table S1 The detail kinetic parameters

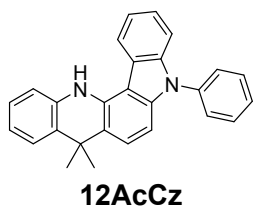
Emitters (Host)	x wt%	ϕ_{PL}^a (%)	ϕ_p/ϕ_D^b (%)	τ_p/τ_d^c (ns)/(μs)	k_{PF}^d (10^7 s $^{-1}$)	k_{DF}^d (10^4 s $^{-1}$)	k_{ISC}^d (10^7 s $^{-1}$)	k_{RISC}^d (10^5 s $^{-1}$)	$k_{r}^{S,d}$ (10^7 s $^{-1}$)	$k_{nr}^{S,d}$ (10^6 s $^{-1}$)	Φ_{ISC}^d (%)
23AcCz-PM^e (DPEPO)	10	95	58/37	14/3.4	4.2	10.8	1.6	1.8	2.4	1.3	38.8
	20	91	52/39	17/4.5	3.1	8.6	1.3	1.5	1.60	1.6	42.7
	30	90	50/40	23/4.6	2.2	8.7	0.97	1.6	1.1	1.2	44.4

^a Absolute PL quantum yield measured with integrating spheres; ^b According to the prompt and delayed components in transient delay curves.; ^c Fitted transient PL curve of prompt and decay components; ^d calculated using equations S1-S7; ^e data from Fig. 5b;

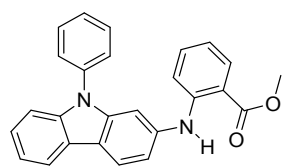
The synthesis of this series of acridine–carbazol hybrid donor was cited by the previous reports.^{7,8} The related ¹H-NMR data of intermediate were also provided.



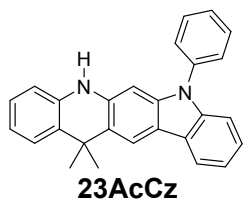
Scheme S1 (a) Pd(OAc)₂, Xantphos, Cs₂CO₃, Toluene, N₂, refluxed, 24 h; (b) CH₃ClMg, dry tetrahydrofuran (THF), N₂, room temperature, overnight; (c) AcOH, HCl, refluxed 12 h.



¹H NMR (600 MHz, DMSO-*d*₆) δ = 8.72 (d, *J* = 7.6, 1H), 8.24 (s, 1H), 7.69 (td, *J* = 10.1, 7.9, 4.0, 2H), 7.65–7.59 (m, 2H), 7.59–7.53 (m, 1H), 7.52–7.38 (m, 4H), 7.33 (dt, *J* = 15.9, 6.3, 2H), 7.21–7.12 (m, 1H), 6.99–6.89 (m, 1H), 6.88–6.80 (m, 1H), 1.62 (d, *J* = 6.6, 6H)



¹H NMR (600 MHz, DMSO-*d*₆) δ 9.43 (s, 1H), 8.25–8.09 (m, 2H), 7.87 (dd, *J* = 8.0, 1.6 Hz, 1H), 7.72–7.58 (m, 4H), 7.51 (ddt, *J* = 8.6, 7.2, 1.5 Hz, 1H), 7.42–7.23 (m, 5H), 7.19 (d, *J* = 7.4 Hz, 2H), 6.78 (ddd, *J* = 8.1, 7.0, 1.1 Hz, 1H), 3.83 (s, 3H).



¹H NMR (600 MHz, DMSO-*d*₆) δ = 9.05 (s, 1H), 8.23 (s, 1H), 8.14 (d, *J*=7.6, 1H), 7.70 (t, *J*= 7.8, 2H), 7.67–7.61 (m, 2H), 7.58–7.50 (m, 1H), 7.41 (dd, *J*= 7.8, 1.3, 1H), 7.28 (dd, *J*= 6.0, 1.4, 2H), 7.21 (ddd, *J*= 7.9, 5.9, 2.2, 1H), 7.06 (td, *J*= 7.5, 1.4, 1H), 6.87–6.79 (m, 2H), 6.76 (dd, *J*= 7.9, 1.3, 1H), 1.63 (s, 6H).

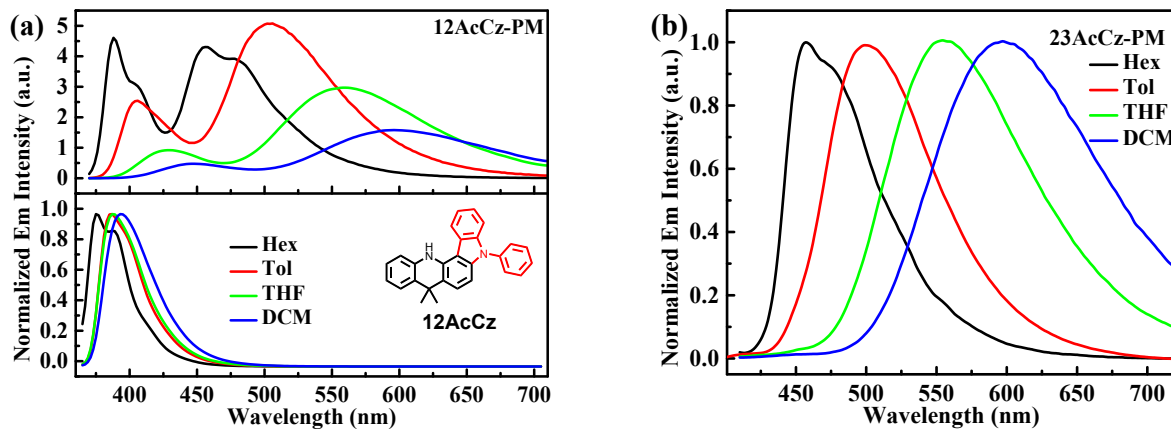


Fig. S1 The emission spectra in different solvents for 12AcCz (1.0 × 10⁻⁵ M), 12AcCz-PM (1.0 × 10⁻⁵ M) (a) and 23AcCz-PM (b).

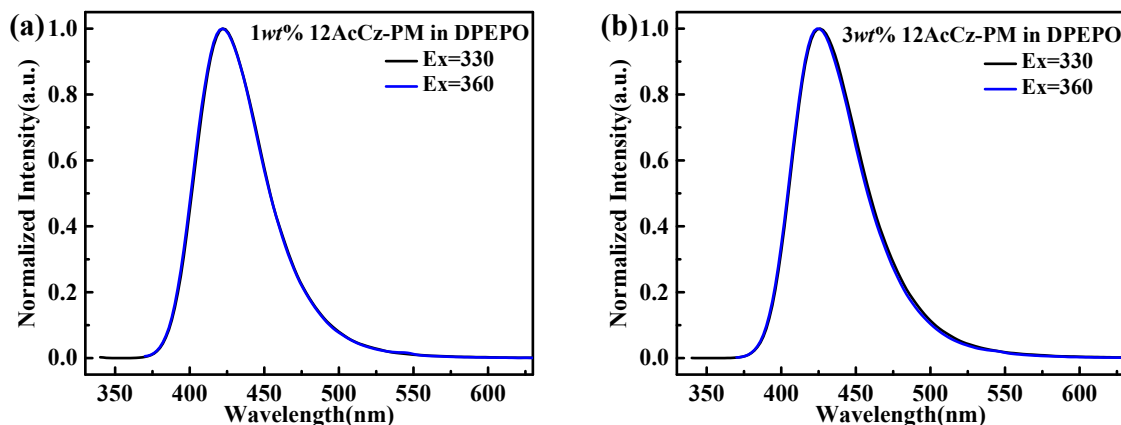
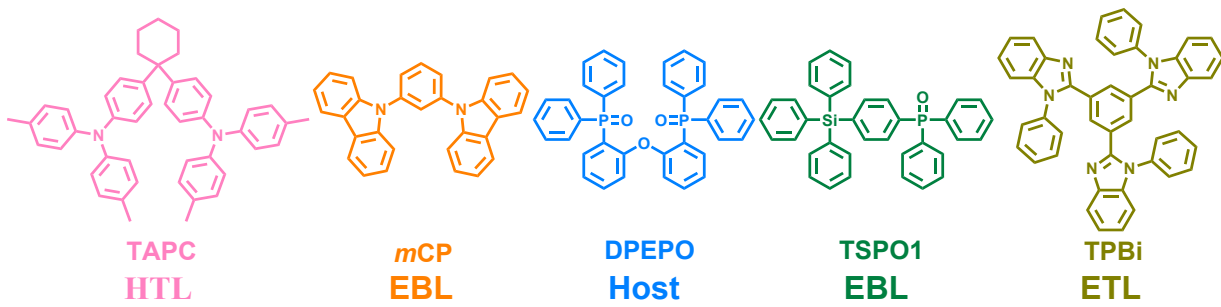


Fig. S2 Fluorescence (300 K) *x* wt% 12AcCz-PM doped in DPEPO films (*x*=1 and 3).

The description for the full name and function of the material in device fabrication was provided as follows:

TAPC: 1,1-bis[4-[*N,N*-di(*p*-tolyl)-amino]phenyl]-cyclohexane; TPBi: 1,3,5-tris(1-phenyl-1*H*-benzo[*d*]imidazol-2-yl)benzene; *m*CP: 1,3-di(9*H*-carbazol-9-yl)benzene; TSPO1: diphenyl(4-(triphenylsilyl)phenyl)phosphine oxide; DPEPO:(oxybis(2,1-phenylene))bis(diphenylphosphine oxide). PEDOT: PSS and LiF acted as hole- and electron-injecting layers, respectively.



Scheme S2 The molecular structure and function of the material in device fabrication (HTL: hole-transporting layers; EBL: exciton blocking layer; ETL: electron-transporting layers.)

To confirm the improved horizontal dipole orientation, the transition dipole moments were calculated by TD-DFT B3LYP/6-31+G(d,p) for the lowest transition from the ground (S_0) to the excited state (S_1). It is found that the dipole moments are basically along their long axis in most cases.^{9, 10} Such relatively linear dipole moments of **12AcCz-PM** and **23AcCz-PM** might facilitate extra photons output from devices.

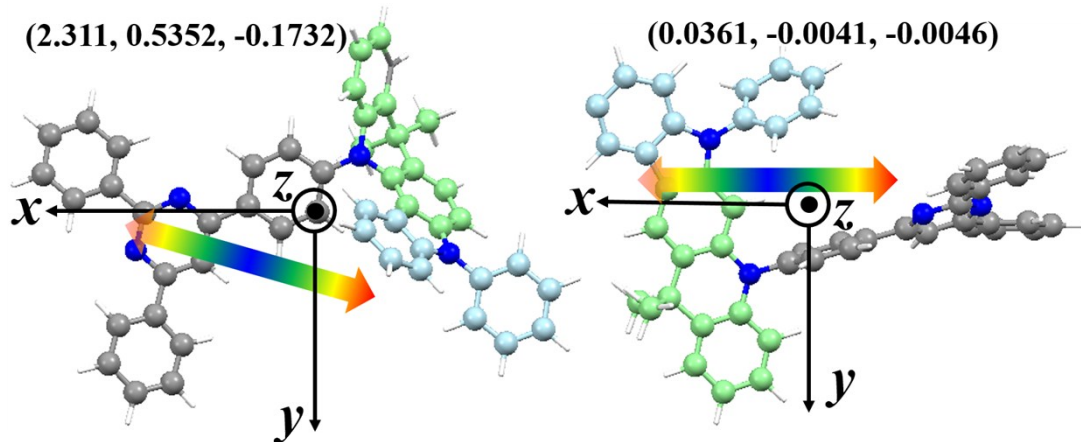


Fig. S3 The direction of the calculated transition dipole moment (as indicated by arrow) of **12AcCz-PM** and **23AcCz-PM** relative to the coordinate of the molecular structure.

The TTA mode simulation can be described as follow:^{11, 12}

$$\frac{\eta_{ext}^{TT}(J)}{\eta_0} = \frac{J_0}{4J} \left(\sqrt{1 + \frac{8J}{J_0}} - 1 \right)$$

where η , η_0 , and J_0 represent the EQE in the presence of TTA, initial EQE in the absence of TTA (at very low current densities, rendering the TTA quenching negligible), and the current density at the half-maximum of the EQE, respectively.

Moreover, the SPA model, which can be expressed by Equation:^{11, 12}

$$\frac{\eta_{ext}^{SP}(J)}{\eta_0} = \frac{1}{1 + (\frac{J}{J_0})^{\frac{1}{l+1}}}$$

Where η_{ext}^{SP} is the EQE in the presence of SPA and l is the fitting parameter.

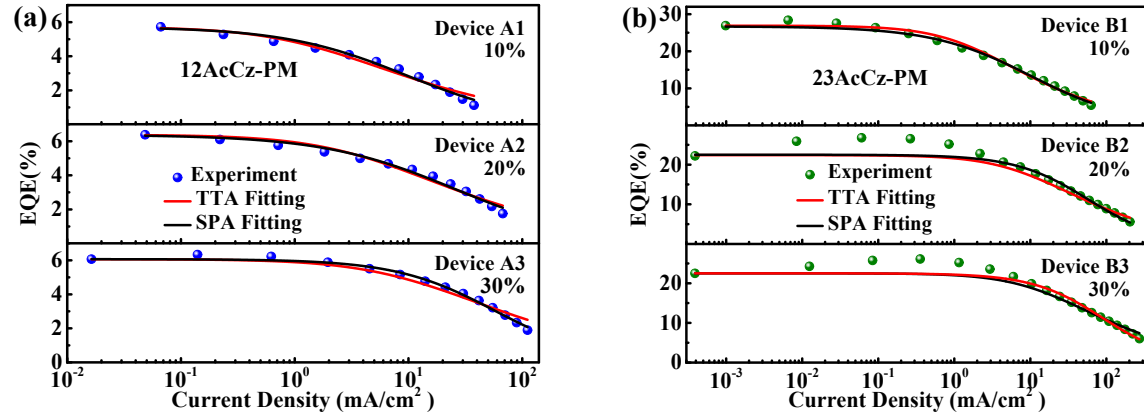


Fig. S4 The external quantum efficiency (EQE) as a function of current density and the fitting results according to TTA and SPA.

References

1. S. Kothavale, K. H. Lee and J. Y. Lee, *ACS Appl. Mater. Interfaces*, 2019, **11**, 17583-17591.
2. Y. J. Kang, J. H. Yun, S. H. Han and J. Y. Lee, *J. Mater. Chem. C*, 2019, **7**, 4573-4580.
3. J. G. Yu, S. H. Han, H. L. Lee, W. P. Hong and J. Y. Lee, *J. Mater. Chem. C*, 2019, **7**, 2919-2926.
4. Q. Zhang, S. Sun, X. Lv, W. Liu, H. Zeng, R. Guo, S. Ye, P. Leng, S. Xiang and L. Wang, *Mater. Chem. Front.*, 2018, **2**, 2054-2062.
5. X. Lv, W. Zhang, D. Ding, C. Han, Z. Huang, S. Xiang, Q. Zhang, H. Xu and L. Wang, *Adv. Opt. Mater.*, 2018, **6**, 1800165.
6. X. Lv, R. Huang, S. Sun, Q. Zhang, S. Xiang, S. Ye, P. Leng, F. B. Dias and L. Wang, *ACS Appl. Mater. Interfaces*, 2019, **11**, 10758-10767.
7. S. G. Yoo, W. Song and J. Y. Lee, *Dyes Pigm.*, 2016, **128**, 201-208.
8. Q. Zhang, S. Sun, W. Liu, P. Leng, X. Lv, Y. Wang, H. Chen, S. Ye, S. Zhuang and L. Wang, *J. Mater. Chem. C*, 2019, 9487.
9. M. Liu, R. Komatsu, X. Cai, K. Hotta, S. Sato, K. Liu, D. Chen, Y. Kato, H. Sasabe, S. Ohisa, Y. Suzuri, D. Yokoyama, S.-J. Su and J. Kido, *Chem. Mater.*, 2017, **29**, 8630-8636.
10. T. Lee, B. Caron, M. Stroet, D. M. Huang, P. L. Burn and A. E. Mark, *Nano Lett.*, 2017, **17**, 6464-6468.
11. S.-F. Wu, S.-H. Li, Y.-K. Wang, C.-C. Huang, Q. Sun, J.-J. Liang, L.-S. Liao and M.-K. Fung, *Adv. Funct. Mater.*, 2017, **27**, 1701314.
12. S. Reineke, K. Walzer and K. Leo, *Phys. Rev. B*, 2007, **75**, 125328.